The Nrf2-ARE Pathway Is Associated With Schisandrin B Attenuating Benzo(a)pyrene-Induced HTR Cells Damages *in Vitro*

Qulong Dong,[1] Haiyan Hou,[1,2] Jun Wu,[3] Yaqiong Chen[1,4]

[1]Department of Obstetrics and Gynecology, Affiliated Hospital of Logistics University of the Chinese People's Armed Forces, Tianjin 300162, China

[2]Chinese Academy of Medical Sciences & Peking Union Medical College, Beijing 100730, China

[3]Program in Public Health and Department of Epidemiology, University of California, Irvine, 92697, USA

[4]Tianjin Key Laboratory for Prevention and Control of Occupational and Environmental Hazard, Tianjin 300162, China

Received 3 March 2015; accepted 11 April 2015

ABSTRACT: As is ubiquitous in the environmental sources, benzo(a)pyrene (BaP) has been reported to induce reprotoxicity in previous studies. Toxicity to trophoblast cells may be one key factor, but evidences were absent. We speculated that BaP can induce cytotoxicity in human trophoblast HTR-8/SVneo (HTR) cells, and Schisandrin B (Sch B) as a potential protector can inhibit the cytotoxicity. MTS assay identified that BaP induced HTR cells death while Sch B played a cytoprotective role. And after Nrf2 interference, the ability of Sch B-induced cytoprotection was declined. Furthermore, PCR, western blot, ELISA, and SOD assays were found that Sch B significantly increased the mRNA and protein expression of Nrf2, HO1, NQO1, and SOD in the Nrf2-ARE pathway, and the extents of increase were declined after Nrf2 interference. These results demonstrated that the Nrf2-ARE pathway plays an important role in Sch B attenuating BaP-induced HTR cells damages *in vitro*. © 2015 Wiley Periodicals, Inc. Environ Toxicol 00: 000–000, 2015.
Keywords: benzo(a)pyrene; Schisandrin B; Nrf2-ARE pathway; HTR

INTRODUCTION

As one of the polycyclic aromatic hydrocarbons (PAHs), benzo(a)pyrene (BaP) is produced by incomplete combustion, and is ubiquitous in the environmental, dietary and occupational sources (Lewtas et al., 2007; Nerbert et al., 2013). BaP has received much attention due to its carcinogenic and mutagenic potential. Evidences that BaP can also induce reprotoxicity in mouse and human being have emerged in recent years. It is reported that BaP can induce significant DNA damage in mouse oocytes and cumulus cells (Einaudi et al., 2014). Previous study demonstrated that BaP exposure for pregnant rats predisposed offspring to functional deficits in cardiovascular system development (Jules et al., 2012). In human being, many studies have identified that BaP is adversely associated with placental weight and cord length (Al-Saleh et al., 2013), and high levels of benzo[a]pyrene-7,8-diol-9,10-epoxide-DNA (BPDE-DNA) adducts in maternal and cord blood are positively associated

Correspondence to: Y. Chen; e-mail: chenyq82@hotmail.com

Contract grant sponsor: National Natural Science Foundation of China.

Contract grant number: 81273977.

Yaqiong Chen conceptualized the study and was the PI in the project. Haiyan Hou was in charge of experiment design, method development, and study coordination. Qulong Dong conducted the experiments, performed the statistical analysis, and wrote the first draft of the paper. Jun Wu contributed mainly to paper revision. All authors have participated in paper writing, and have read and approved the final manuscript.

Published online 00 Month 2015 in Wiley Online Library (wileyonlinelibrary.com). DOI: 10.1002/tox.22149

with symptoms of anxiety, depression and attention problems in children at the age of 6-7 (Perera et al., 2012). As the metabolite of BaP, BPDE usually induces DNA damage by binding to DNA to form mutagenic BPDE-DNA adducts (Lacoste et al., 2010). Additionally, our group has previously found that high levels of maternal BaP exposure may contribute to an increased risk of miscarriage during early pregnancy (Wu et al., 2010).

Trophoblast cells are an essential for normal pregnancy because of its invasion into uterus, and its regulatory role in maternal-fetal exchange as well. Previous study has identified that BaP can inhibit the proliferation of trophoblast cell lineages in mouse (Xie et al., 2010). Another study related to DNA damage in human placenta from smoking and nonsmoking women, which has found that BPDE-DNA adducts located in the nuclei of cytotrophoblast cells and syncytiotrophoblast knots exists in the chorionic villi (Pratt et al., 2011). Therefore, we speculated that toxicity to trophoblast cells may be one of key mechanisms induced by BaP. The present study aim is to examine the direct influence of BaP on human trophoblast cells by using the HTR cell line *in vitro*.

Nrf2 belongs to the Cap'n'collar family of basic leucine zipper transcription factor (Li et al., 2009). Under normal conditions, Nrf2 is sequestered by kelch ECH associating protein 1 (KEAP1) in the cytoplasm and remains inactive. However, Nrf2 can be activated via releasing from KEAP1 and translocating into the nucleus under certain circumstances (such as oxidative stress) (Kensler et al., 2007). Activated Nrf2 can bind to antioxidant response element (ARE) to trigger the Nrf2-ARE pathway and subsequently activate downstream protective genes and enzymes including NAD(P)H:quinine oxidoreductase 1 (NQO1), heme oxygenase-1 (HO1), glutathione, glutathione S-transferase, superoxide dismutase (SOD), and so on (Ding et al., 2014; Satoh et al., 2014). The Nrf2-ARE pathway has been identified to be the pivotal regulator for oxidative stress, which participates in many physiological and pathological processes, it also plays an important role on anti-tumor, anti-aging, anti-inflammatory, anti-apoptosis as well as against cells injury (Pakala et al., 2010; Leong et al., 2011; Luo et al., 2011; Singh et al., 2013). Previous study demonstrated that Nrf2 can up-regulate the expression of antioxidant enzyme genes, including SOD and glutathione peroxidase, and consequently inhibit trophoblast cells apoptosis induced by dexamethasone in pregnant rats (Lin et al., 2013). Another study found that Nrf2 activation and subsequent expression of HO1 and NQO1 can protect human keratinocytes from BaP-induced damage (Wu et al., 2014). Therefore, we speculate that Nrf2 activation may protect HTR cells from BaP-induced damage.

Traditional Chinese drug Five-Seed Procreating Pill has been found to improve fertility in humans. Schisandra chinensis, the principal component of the drug, is a commonly-used Chinese herb for promoting health, and it is also clinically prescribed to treat viral and chemical hepatitis (Liu et al., 1989). As the most abundant and active dibenzocyclooctadiene lignan isolated from Schisandra chinensis, Schisandrin B (Sch B) has been reported to activate Nrf2 and downstream glutathione against oxidant stress and cells apoptosis (Chiu et al., 2011; Leong et al., 2011; Leong et al., 2012). It was found Sch B can induce nuclear translocation of Nrf2, increase the transcription of its dependent genes, and subsequently exhibit anti-inflammatory activity in lymphocytes (Checker et al., 2012).

Although no study indicated the role of Sch B on HTR cells damages. We speculate that Sch B can attenuate BaP-induced HTR cells damages via activating the Nrf2-ARE pathway. For the first time, we directly investigated the BaP-induced cytotoxicity and Sch B-induced cytoprotection by using HTR cells model *in vitro*. Moreover, in order to explore the potentially protective role of Nrf2-ARE pathway, the transfection with small interfering RNA (SiRNA) targeting Nrf2 was performed in this study.

ABBREVIATIONS

ARE	antioxidant response element
BaP	benzo(a)pyrene
BPDE	benzo[a]pyrene-7,8-diol-9,10-epoxide
DMSO	dimethyl sulphoxide;
HO1	heme oxygenase-1
NQO1	NAD(P)H:quinine oxidoreductase 1
Sch B	Schisandrin B
SiRNA	small interfering RNA; SOD, superoxide dismutase

MATERIALS AND METHODS

Materials

The HTR cell line was obtained from Professor Graham CH from University of Toronto, Canada. BaP (≥96% purity) and Sch B (≥98% purity) were obtained from the National Institutes for Food and Drug Control of China. Nrf2 SiRNA and SiRNA transfection reagent were purchased from Santa Cruz Biotechnology (Santa Cruz, CA). RPMI-1640 medium and fetal bovine serum (FBS) were purchased from Gibco (Gibco, Grand Island, USA). MTS Cell Proliferation Assay reagent was purchased from Promega (Beijing) Biotech, Ltd. (Promega, Beijing, China). Primers for PCR were provided by Beijing Dingguo Changsheng Biotechnology Co., Ltd. (Dingguo, Beijing, China). Primary rabbit monoclonal antibody (anti-Nrf2, anti-HO1, anti-NQO1, anti-β-actin, and anti-Lamin B1) and secondary antibody (goat anti-rabbit IgG) were purchased from Abcam Company (Abcam, Cambridge, UK). ELISA kits for HO1 and NQO1 protein examination were obtained from Shanghai BlueGene Biotech (BlueGene, Shanghai, China). SOD activity assay kit for T-SOD activity examination was purchased from Cell Biolabs

(Cell Biolabs, CA). Protein extraction kits for total protein and nuclear and BCA Protein Assay Kit were purchased from Applygen Technologies (Applygen, Beijing, China).

Cell Culture

The HTR cell line was cultured in RPMI-1640 medium supplemented with 10% FBS and 1% penicillin/streptomycin under 37°C in a humidified atmosphere with 5% CO_2. Cells were usually grown at almost 70% of confluence before the exposure to Sch B and/or BaP in the various experiments.

MTS Cell Proliferation Assay

To detect the BaP-induced cytotoxicity, we firstly culture cells in a 96-well plate at a density of 0.5×10^4 cells/well. After incubation for 24 h, the cells in BaP treatment groups were respectively treated with 1, 2.5, 5, 10, 20, and 40 μM BaP dissolved in the vehicle dimethyl sulphoxide (DMSO) while cells in the control group were treated with 0.1% vehicle DMSO. After 24 h incubation, 20 μL MTS and 100 μL RPMI-1640 medium supplemented with 10% FBS were used to replace the previous medium in every well for a 2.5 h incubation at 37°C. Then the absorbance values at 492 nm were measured using an enzyme-linked immunosorbent detector (Thermo, USA). This MTS assay was performed in triplicates. We chose the concentration of 20 μM BaP in the latter experiments because of its appropriate cell inhibition rate (28.1% cell inhibition rate compared with the control).

Next step, we examined the effect of Sch B alone treatment on HTR cells. Cells were treated with 0.25, 0.5, 1, 2, 5, and 10 μM Sch B dissolved in the DMSO, while the control cells were treated with 0.1% vehicle DMSO only. After 24 h incubation, MTS cell proliferation assay was applied as described above in triplicate. Moreover, in order to detect the protective effect of Sch B against BaP, cells in Sch B combining with BaP groups were treated with 0.25, 0.5, 1, 2, 5, and 10 μM Sch B 6 h before 20 μM BaP treatment, while cells from BaP-only group were treated with 20 μM BaP alone, and the control cells were treated with 0.1% vehicle DMSO. Compared with the BaP-only group, exposure to 0.5, 1 and 2 μM Sch B combining with BaP groups induced relative bigger cytoprotection rates than other Sch B combining with BaP groups (the three cytoprotection rates compared with BaP-only group were 10.4%, 19.1%, and 24.0%, respectively). Thus we chose to use 0.5, 1, and 2 μM Sch B in the latter experiments.

Nrf2 Interference, Interference Efficiency Analysis, and MTS Cell Proliferation Assay after Nrf2 Interference

Cells were cultured at 37°C in 2 mL antibiotic-free normal growth medium supplemented with 10% FBS at a density of 1.5×10^5 cells per well in a 6-well plate. After 24 h, the cells grown at 70% of confluence were transfected with Nrf2 SiRNA and scrambled SiRNA according to the siRNA transfection protocol. Five groups were respectively treated with 0.25 μg Nrf2 SiRNA, 0.5 μg Nrf2 SiRNA, 1 μg Nrf2 SiRNA, 0.5 μg scrambled SiRNA (the negative control group) and without SiRNA (the control group). RNA interference efficiency for each group was measured by real-time PCR and western blot after 36 h of transfection.

Then, total RNA was isolated, and total protein was extracted from the five groups described above, respectively. Total RNA was used for reverse transcription to cDNA samples, which were amplified by real-time PCR, while total protein was used for western blot. Interestingly, both real-time PCR and western blot showed agreement on 1 μg Nrf2 SiRNA transfection for the optimal interference efficiency (interference efficiency was 74.9% and 81.3% in real-time PCR and western blot analyses compared with the control group, respectively). Hence we decided to choose 1 μg Nrf2 SiRNA to transfect cells in the latter experiments which needed Nrf2 interference.

After 1 μg Nrf2 SiRNA transfection, we again examined the cytoprotective effect of Sch B against BaP. Briefly, cells after 36 h transfection of 1μg Nrf2 SiRNA were divided into five groups including the control group, 20 μM BaP-only group, and groups with 0.5, 1, and 2 μM Sch B treatment 6 h before 20 μM BaP treatment. After 24 h incubation, MTS assay was applied in triplicates as above.

Groups Division in Subsequent Experiments

Subsequent experiments including PCR, western blot analysis, Elisa assay, and SOD activity assay were conducted in cells without Nrf2 interference (before Nrf2 interference) and conducted again in cells with Nrf2 interference (after Nrf2 interference). With and without Nrf2 interferences, the cells in these experiments were divided into five groups including the control group (cells were treated with 0.1% DMSO only), BaP-only group (cells were treated with 20 μM BaP), and three Sch B combining with BaP groups (cells were treated with 0.5, 1 and 2 μM Sch B 6 h before 20 μM BaP treatment). Sch B and BaP were dissolved in DMSO as above.

RNA Isolation and cDNA Synthesis

Both with and without Nrf2 SiRNA interferences, five groups of cells were respectively treated with 0.1% DMSO, 20 μM BaP only and 0.5, 1, 2 μM Sch B 6 h before 20 μM BaP treatment as above. After 24 h incubation, total RNA from the five groups of cells was isolated by using the TRIzol reagent (Invitrogen, CA) before and after Nrf2 SiRNA transfection. Subsequently, the isolated RNA was reversely transcribed to cDNA samples by using Quant script RT Kit

(Tiangen Biotech, Beijing, China) following up manufacturer's instructions.

Real-Time Polymerase Chain Reaction (real-Time PCR)

Real-time PCR was performed in a real-time 7500 PCR system (Applied Biosystems, CA, USA) using TransStart Top Green qPCR SuperMix (Transgen Biotech, Beijing, China) with the cDNA samples. Polymerase activation was performed at 95°C for 10 min, followed by 40 cycles of denaturing at 95°C for 30 s, annealing at 60°C for 34 s and extension at 72°C for 45 s. The amount of target gene mRNA was normalized to the level of GAPDH mRNA. Each experiment was repeated three times. Primers specific for Nrf2, HO1, NQO1, SOD, KEAP1 and GAPDH were listed as below. Nrf2: forward:5'-GGCATCACCAGAACACTCAG-3'; Reverse: 5'-TGACCAGGACTTA CAGGC AAT-3'; HO1: forward:5'-CAAGCCGAGAATGCTGAGT TCATG-3'; Reverse: 5'-GCAAGGGATGATTTCCTG CCAG-3'; NQO1: forward:5'-TATCCTGCCGAGTCTGTTC TG-3'; Reverse: 5'-AACTGGAATATCACAAGGTCTG C-3'; SOD: forward:5'-GCCGATGTGTCTATTGAAGAT TC-3'; Reverse: 5'-AGCAGGATAACAGATGAGTTAAG G-3'; KEAP1: forward:5'-CAGAGGTGGTGGTGTTGCTTAT-3'; Reverse:5'-AGCTCGTTCATGATGCCAAAG-3'; GAPDH: forward:5'-AGGGGTCTACATGGCAACTG-3'; Reverse:5'-CGACCACTTTGTCAAGCTCA-3'.

Reverse Transcription Polymerase Chain Reaction (RT-PCR)

The PCR amplification of the cDNA samples were performed using a Perkin Elmer Applied Biosystems GeneAmp PCR System 9600 (Applied Biosystems, CA). The PCR conditions were the same as real-time PCR and the products were subjected to 2% agarose gels and stained with ethidium bromide.

Western Blot Analysis

Both before and after Nrf2 SiRNA transfection, total protein and nucleoprotein were extracted from the five groups of cells using the specific kit according to the manufacturer's protocol. Protein concentration was determined using the BCA Protein Assay Kit and an equal amount of protein (50 μg) for each sample was separated by 8% or 12% sodium dodecylsulfate-polyacrylamide gel electrophoresis. Target proteins were transferred to polyvinylpyrrolidine difluoride membranes and blocked by 5% fat-free milk for 1 h. Protein detection was performed by incubating primary antibody overnight at 4°C, followed by incubation 1 h at 37°C with HRP conjugated secondary antibody. Detection of secondary antibody was performed using the ECL Western Blotting Detection Reagents (advansta, CA). Total protein was used for detecting the expression of Nrf2, HO1, NQO1 and β-actin, while nucleoprotein was used for detecting Nrf2 and Lamin B1 expression.

Elisa Assay

Both before and after Nrf2 SiRNA transfection, NQO1 and HO1 proteins from five groups of cells medium supernatant were examined using specific ELISA Kit following the manufacturer's protocol. Then, the optical density of each well was determined at 450 nm using an enzyme-linked immunosorbent detector (Thermo, USA). Each group was made in triplicate and this assay was repeated for three times.

SOD Activity Assay

Both before and after Nrf2 SiRNA transfection, the medium supernatant T-SOD activity from five groups was detected using the SOD Assay Kit following up the instruction. Each group was made in triplicate and this assay was repeated three times.

Statistical Analysis

All data were quantitative and were analyzed using a one-way analysis of variance (ANOVA) with SPSS 13.0 software (SPSS, USA). The difference was considered to be statistically significant at $P < 0.05$.

RESULTS

BaP Induced Cytotoxicity and Sch B Exerted Cytoprotection against BaP in HTR Cells

As observed in Figure 1(A), all six groups treated with different concentrations of BaP alone induced significant cytotoxicity as compared with the control group ($P < 0.01$). Since the group with 20 μM BaP treatment induced a suitable cytotoxicity for further study (28.1% inhibition rate compared with the control group), we chose this concentration as fixed BaP-induced cytotoxicity model in latter experiments. Next, we detected the effects of different concentrations of Sch B alone in HTR cells. As shown in Figure 1(B), all concentrations of Sch B alone did not induced cytotoxicity except for the 10 μM Sch B as compared with the control group. And interestingly, the Sch B at the concentration of 0.5, 1 and 2μM induced a mild HTR cells proliferation as compared with the control group. In Figure 1(C), we could see that all groups treated with different concentrations of Sch B 6 h before 20 μM BaP treatment induced cytoprotection as compared with 20 μM BaP-only group ($P < 0.01$) except the 10 μM Sch B combining with BaP treatment group induced a stronger cytotoxicity than BaP-only group ($P < 0.01$). Also, Figure 1(C) showed that although Sch B treatment groups showed lower cell proliferation rate than the control, the groups with 0.5, 1, and 2 μM Sch B treatment significantly largely decreased cytotoxicity induced by BaP ($P < 0.01$).

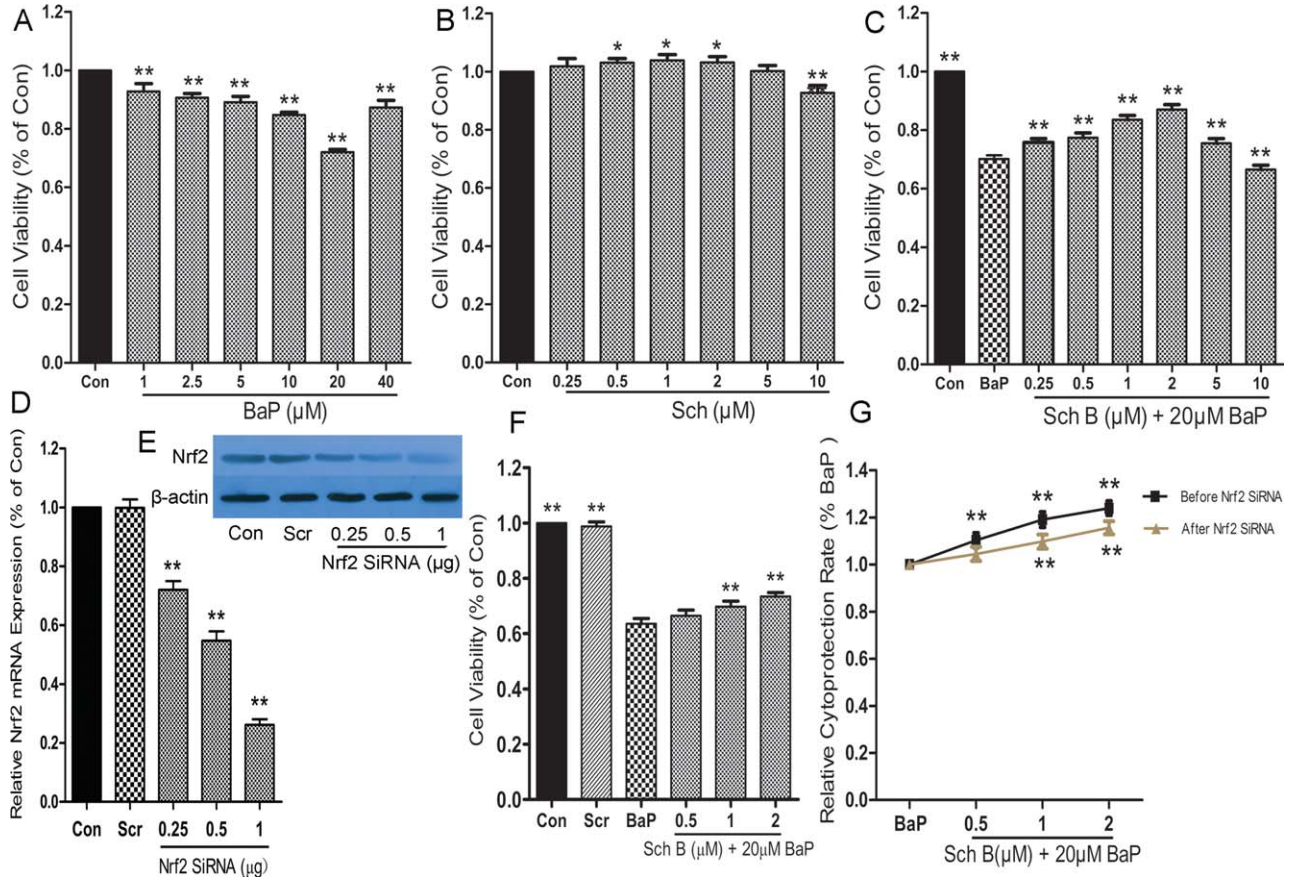

Fig. 1. BaP and Sch B induced cytotoxicity and cytoprotection in HTR cells respectively. MTS assay was performed to detect cell proliferation at different concentrations of BaP alone (A), Sch B alone (B) and Sch B 6 h before 20 μM BaP treatment (C). Real-time PCR (D) and Western bolt (E) were performed to explore the inference efficiency of Nrf2 mRNA. MTS assay was performed again to detect protective effect of Sch B 6 h before 20 μM BaP treatment after Nrf2 interference (F). Analysis of relative cytoprotection rate of Sch B compared with BaP-only was conducted (G). Results were analyzed as mean ± STD using the one-way ANOVA. A-F: * $P < 0.05$ versus Con; ** $P < 0.01$ versus Con; G: ** $P < 0.01$ versus BaP. 54 x 37 mm (600 x 600 DPI). [Color figure can be viewed in the online issue, which is available at wileyonlinelibrary.com.]

Nrf2 Interference Increased BaP-Induced Cytotoxicity and Decreased Cytoprotection of Sch B against BaP in HTR Cells

Figure 1(D,E) clearly showed that compared with the control group, scrambled group did not interfere in Nrf2 expression, but Nrf2 SiRNA transfection groups significantly decreased expression of Nrf2 in both mRNA ($P < 0.01$) and protein ($P < 0.01$) level through a dose-effect relation. Among them, 1 μg Nrf2 SiRNA transfection led to 74.9% Nrf2 mRNA interference rate and 81.3% Nrf2 total protein interference rate as compared with the control group through real-time PCR and western blot analysis, respectively. Taking the almost 75% interference efficiency into consideration, we decided to use 1 μg Nrf2 SiRNA with latter transfection.

As observed in Figure 1(F,G), after Nrf2 SiRNA transfection, the cytotoxicity induced by BaP increased significantly (cell inhibition rate added to 36.4% as compared with the control group, $P < 0.01$). In addition, the cytoprotection rate in 0.5, 1 and 2 μM Sch B combining with BaP groups significantly decreased to 4.5%, 9.8% and 15.6% as compared with the BaP-only group respectively, while the cytoprotection rate before Nrf2 SiRNA transfection was 10.4%, 19.1%, and 24.0%, respectively.

Sch B Significantly Increased Nrf2, Ho1, Nqo1, and SOD mRNA Expression before and after Nrf2 Interference and Nrf2 Interference Reduced the Amount of Increase

Figure 2(A–E) showed the relative mRNA expression (% of the control group) in real-time PCR. Both before and after Nrf2 interference, BaP-only treatment group slightly increased Nrf2 mRNA expression as compared with the control group ($P < 0.05$), while 0.5, 1, and 2 μM Sch B combining with BaP treatment groups significantly activated Nrf2

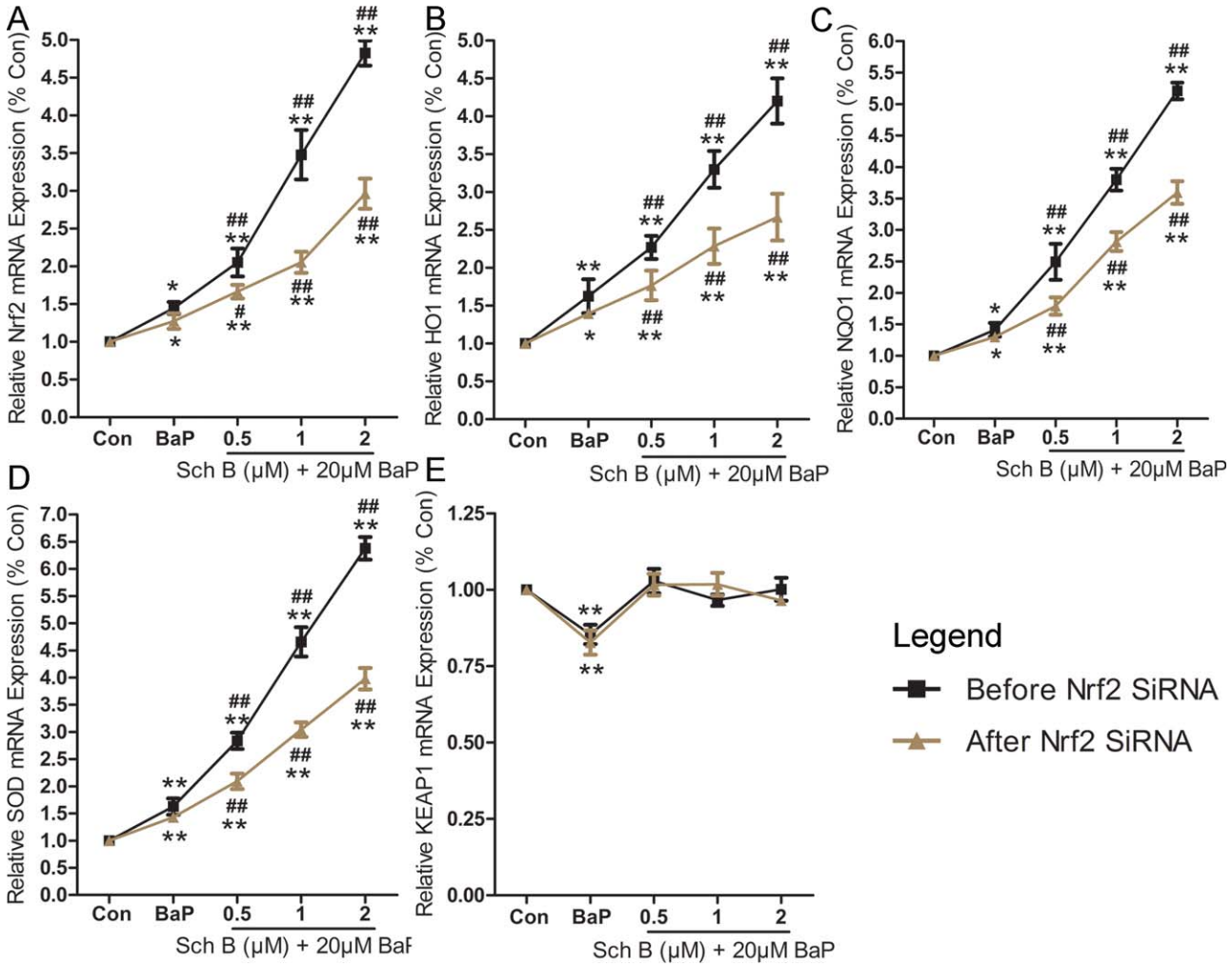

Fig. 2. Sch B significantly increased Nrf2, HO1, NQO1 and SOD mRNA expression before and after Nrf2 interference and Nrf2 interference reduced the amount of increase in real-time PCR. (A), (B), (C), (D) and (E) were relative mRNA expression of Nrf2, HO1, NQO1, SOD, and KEAP1 in real-time PCR analyses respectively. Data were calculated using 2-ΔΔCT and analyzed as mean ± STD using the one-way ANOVA. * $P < 0.05$ versus Con; ** $P < 0.01$ versus Con; # $P < 0.05$ versus BaP; ## $P < 0.01$ versus BaP. 61 x 47 mm (600 x 600 DPI). [Color figure can be viewed in the online issue, which is available at wileyonlinelibrary.com.]

mRNA transcription as compared with both the control group and the BaP-only treatment group through a dose-effect relation in Figure 2(A) ($P < 0.01$). For the downstream genes of Nrf2 including HO1, NQO1 and SOD, we found a similar trend as Nrf2 mRNA expression before and after Nrf2 interference [Fig. 2(B–D)]. Moreover, we could watch a decline in the amount of increase of Nrf2, HO1, NQO1 and SOD mRNA expression induced by Sch B after Nrf2 interference [Fig. 2(A–D)]. In addition, we could see that only BaP but not Sch B statistically significantly decreased KEAP1 (the inhibitor of Nrf2) mRNA expression as compared with the controls before and after Nrf2 interference in Figure 2(E) ($P < 0.01$). Further, the results from RT-PCR (another method to identify mRNA expression) agreed with real-time analyses (Fig. 3).

Sch B Significantly Increased Cellular Protein Level of Nrf2, Ho1 and Nqo1 before and after Nrf2 Interference and Nrf2 Interference Reduced the Extent of Increase

Both before and after Nrf2 interference, we could see that BaP-only group and 0.5, 1, and 2 μM Sch B combining with BaP treatment groups promoted Nrf2 nuclear translocation but the three Sch B groups did much stronger through a dose-effect relation in nucleoprotein [Fig. 4(A)]. We also watched that BaP-only treatment slightly increased Nrf2 protein level ($P < 0.01$), while 0.5, 1, and 2 μM Sch B combining with BaP treatment groups obviously amplified the Nrf2 protein expression through a dose-effect relation in total protein ($P < 0.01$) [Fig. 4(B)]. And the Nrf2-dependent HO1

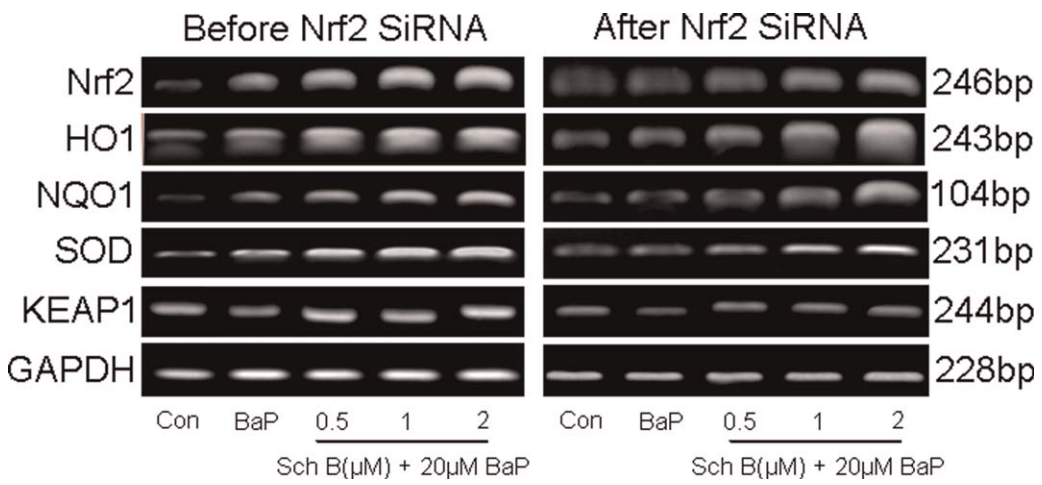

Fig. 3. Sch B significantly increased Nrf2, HO1, NQO1 and SOD mRNA expression before and after Nrf2 interference and Nrf2 interference reduced the amount of increase in RT-PCR analysis. RT-PCR products of Nrf2, HO1, NQO1, SOD, KEAP1 and GAPDH were subjected to agarose gels and stained with ethidium bromide respectively. GAPDH acted as internal control. 60 x 28 mm (300 x 300 DPI).

and NQO1 levels in total protein presented a similar trend as Nrf2 [Fig. 4(B)]. However, after Nrf2 interference, although Sch B combining with BaP groups still significantly increased Nrf2 (both nucleoprotein and total protein), HO1 and NQO1 (total protein) levels through a dose-effect relation ($P < 0.01$) while BaP did slightly ($P < 0.05$), their protein expression levels as well as the extent of increase were noticeably reduced [Fig. 4(A,B)].

Sch B Significantly Increased Ho1, Nqo1 Protein, and T-SOD Activity Level in Medium Supernatant before and after Nrf2 Interference and Nrf2 Interference Attenuated the Extent of Increase

Figure 5(A,B) showed that before and after Nrf2 interference, 0.5, 1, and 2 μM Sch B combining with BaP treatment groups significantly increased HO1 and NQO1 protein levels in medium supernatant through a dose-effect relation as compared with the control group ($P < 0.01$) or BaP-only treatment group ($P<0.01$), but the extent of increase was obviously decreased after Nrf2 interference. Figure 5(C) showed the result of T-SOD activity examination in medium supernatant. Similarly, 0.5, 1 and 2 μM Sch B combining with BaP treatment groups significantly increased T-SOD activity through a dose-effect relation as compared with the control group ($P < 0.01$) or BaP-only treatment group ($P < 0.01$) before and after interference, but the extent of increase was attenuated after Nrf2 interference. Additionally, BaP-only treatment also slightly increased the HO1, NQO1 protein levels and T-SOD activity levels compared with the control group ($P < 0.05$) before and after interference [Fig. 5(A–C)].

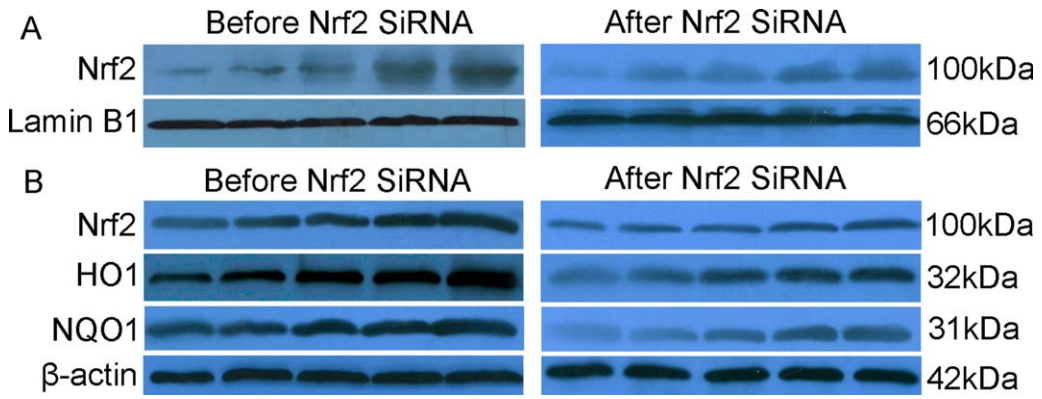

Fig. 4. Sch B significantly increased Nrf2, HO1 and NQO1 level in HTR cells before and after Nrf2 interference and Nrf2 interference attenuated the extent of increase in western blot. Western blot for Nrf2 expression in nucleoprotein (A). Western bolt for Nrf2, HO1 and NQO1 expression in total protein (B). Lamin B1 and β-actin acted as internal control for nucleoprotein and total protein respectively. 25 x 9 mm (300 x 300 DPI). [Color figure can be viewed in the online issue, which is available at wileyonlinelibrary.com.]

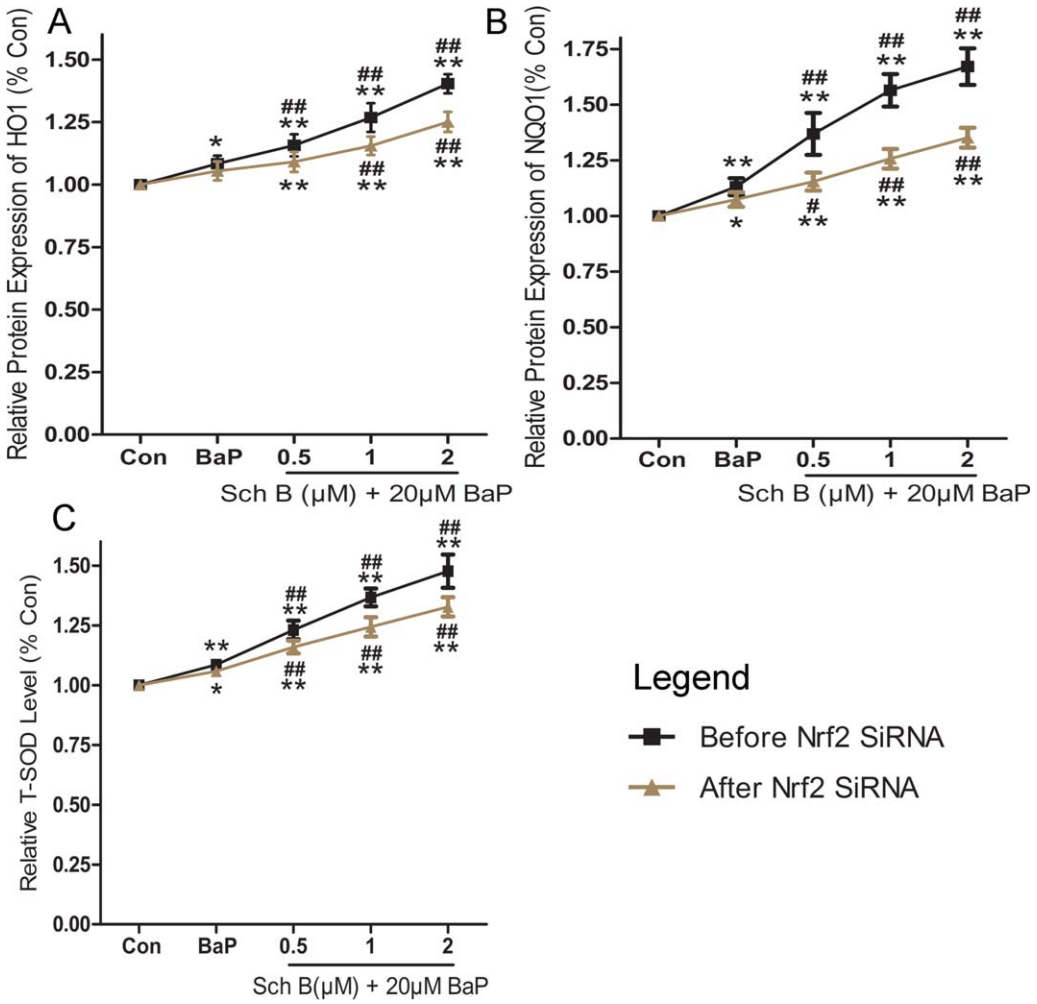

Fig. 5. Sch B signifycantly added the level of HO1, NQO1 protein and T-SOD activity in medium supernatant before and after Nrf2 interference and Nrf2 interference attenuated the extent of increase. (A) and (B) were ELISA for HO1 and NQO1 protein expression in medium supernatant respectively. (C) was SOD assay for T-SOD activity in medium supernatant. All data were analyzed as mean ± SD using the oneway ANOVA. *$P < 0.05$ versus Con; **$P < 0.01$ versus Con; # $P < 0.05$ versus BaP; ## $P < 0.01$ versus BaP. 59 x 57 mm (600 x 600 DPI). [Color figure can be viewed in the online issue, which is available at wileyonlinelibrary.com.]

DISCUSSION

BaP has been recognized for its carcinogenic and mutagenic potential as well as reprotoxicity. Recently, BaP exposure has been associated with adverse pregnancy outcomes such as missed abortion (Tang et al., 2006; Wu et al., 2010). But the underlying pathological mechanism still remains unknown. It has been reported that genetoxic BPDE-DNA adducts exist in the nuclei of the human cytotrophoblast cells and syncytiotrophoblast knots in smoking women (Pratt et al., 2011), and that BaP can inhibit the proliferation of trophoblast cell lineages in mouse (Xie et al., 2010). Being inspired by this, we examined the direct effect of BaP exposure on HTR cells which are essential in normal pregnancy because of their basic functional support for embryo and fetus. We observed that different concentration of BaP induced deaths in HTR cells, especially for 20 μM BaP killing 28.1% HTR cells. To our knowledge, this is the first study reporting the direct cytotoxicity of BaP exposure in HTR cells.

Sch B, the potential cytoprotective reagent against BaP drove our attentions. We found that 0.25, 0.5, 1, 2 and 5 μM Sch B alone did not harm to HTR cells and even 0.5, 1, and 2 μM Sch B alone could slightly induced HTR cells proliferation, but 10 μM Sch B alone did harm to HTR cells. We speculated that low concentration of Sch B (less than 10 μM) had no cytotoxicity in HTR cells, while high concentration of Sch B (no less than 10 μM) could induce cytotoxicity in HTR cells. This speculation was proven in subsequent MTS assay of Sch B combining BaP treatment. In this assay, low concentration of Sch B (especially for 0.5, 1, and 2 μM) exerted a significantly cytoprotective effect against BaP

while 10 μM Sch B combining BaP treatment induced stronger deaths than BaP alone in HTR cells. This is the first study demonstrating that Sch B (less than 10 μM) can attenuate the damage of BaP exposure in HTR cells.

After transfection with 1 μg Nrf2 SiRNA, almost 74.9% Nrf2 mRNA expression was interfered, and then cytotoxicity induced by BaP increased while cytoprotection exerted by 0.5, 1 and 2 μM Sch B declined. It means that Nrf2 play a protective role on Sch B against BaP in HTR cells. It is worth mentioning that Nrf2 is a transcription factor which regulates protective genes against a wide variety of toxic insults to cells (Leinonen et al., 2012). Additionally, a large number studies have reported that Nrf2 can act as a mediator of anti-oxidative stress, anti-tumor, anti-aging, anti-inflammatory, anti-apoptosis as well as against cells injury mainly via activating the Nrf2-ARE signal pathway (Pakala et al., 2010; Leong et al., 2011; Luo et al., 2011; Singh et al., 2013).

However, whether Nrf2-ARE pathway involved in the protective effect of Sch B against BaP remained unknown. In order to explore the role Nrf2-ARE pathway played, the mRNA and protein expression of Nrf2 and downstream genes including HO1, NQO1 and SOD were examined. Both our real-time PCR and RT-PCR results demonstrated that 0.5, 1, and 2 μM Sch B significantly activated Nrf2, HO1, NQO1, and SOD mRNA through a dose-effect relation before and after Nrf2 interference. Western blot analyses suggested that Sch B significantly increased Nrf2 content in nucleoprotein and Nrf2, HO1, and NQO1 content in total protein before and after Nrf2 interference. And the results from ELISA and SOD assay agreed that Sch B significantly and largely augmented the HO1 and NQO1 protein and T-SOD activity in medium supernatant before and after Nrf2 SiRNA transfection. Moreover, as the downstream genes of Nrf2-ARE pathway, HO1, NQO1, and SOD presented a similar trend as the upstream gene Nrf2 in mRNA and protein expression. Results indicated that Nrf2-ARE pathway was activated by Sch B in this study. Further, we also observed that the amount of mRNA and protein expression of Nrf2, HO1, NQO1, and SOD induced by Sch B was declined after Nrf2 interference. In retrospect, the protective effect of Sch B against BaP was much less after Nrf2 interference. We could conclude that Nrf2-ARE pathway played an important role on Sch B attenuating damage of HTR cells exposed on BaP. It was consistent with a former study which found Nrf2 activation and subsequent expression of HO1 and NQO1 could protect human keratinocytes from BaP-induced injury (Luo et al., 2011). Furthermore, as the downstream genes in the pathway, NQO1 activated by Nrf2 had been reported to accelerate BaP detoxification in mouse aortic endothelial cells (Lin et al., 2011). And SOD had been reported to resist BaP-induced toxicity because of its anti-oxidative stress property in rats and mice (Aktay et al., 2011; Sehgal et al., 2012). Although the direct defense of HO1 against BaP has not been studied, HO1 is well known for its anti-oxidative, anti-inflammatory and cytoprotective ability (Bhakkiyalakshmi et al., 2014; Xie et al., 2015). In addition, some studies had also reported that nuclear translocation of Nrf2 could activate the downstream HO1, NQO1, and SOD expression and therefore exert extensive cytoprotection including attenuating cell death, anti-oxidative stress, anti-tumor (Dinkova-Kostova et al., 2013; Wang et al., 2014; Chao et al., 2014).

Unexpectedly, we also observed that BaP slightly activated the Nrf2-ARE pathway. We therefore examined mRNA expression of KEAP1, an inhibitor of Nrf2. Real-time PCR and RT-PCR results showed that BaP but not Sch B downregulated KEAP1 mRNA before and after Nrf2 interference. This was partially consistent with the study which found that BaP could increase Nrf2 content by downregulating the KEAP1 message in Jurkat cells (Nguyen et al., 2010). It has been reported that there are two ways to activate Nrf2, namely by oxidative or covalent modification of KEAP1 and by phosphorylation of Nrf2 (Huang et al., 2002; Xu et al., 2006; Gao et al., 2014). Obviously, BaP activated Nrf2 by downregulating KEAP1 mRNA in our study. We speculated that Sch B most likely activated Nrf2 by phosphorylation of Nrf2. Although this speculation needs to be further studied, it was supported by two previous studies showing that Sch B activated Nrf2 by activating MAPK (especially for ERK) and then Nrf2 phosphorylation in AML 12 hepatocytes and H9c2 cells (Leong et al., 2011; Chiu et al., 2011). However, there seems to be a paradox that BaP slightly activated the cytoprotective Nrf2-ARE signaling pathway while induced cytotoxicity at the same time. Previous literature showed that KEAP1 modification can occur easily with the presence of oxidants and electrophiles (Kansanen et al., 2009). Therefore, BaP likely acted as a powerful oxidant that triggered cellular defense response and activated Nrf2 by downregulating KEAP1 message (Chen et al., 2007; Gao et al., 2011; Ji et al., 2013). Unfortunately, slightly activated Nrf2-ARE pathway did not reverse the excessive cytotoxicity induced by BaP.

Based on our results in cells, genes and protein aspects, we conclude that the Nrf2-ARE pathway plays an important role on Sch B attenuating HTR cells damage exposed on BaP *in vitro*. To our knowledge, this was the first study that demonstrates the protective effect of Sch B on HTR cells against the direct damage from BaP exposure. Our results provide new and meaningful insights into protecting human reproduction from injury induced by PAHs.

The authors thank Hong Chen and Bo Cao (Department of Pharmacognosy, Logistics College of the Chinese People's Armed Police Forces) to provide excellent technical assistance. Thanks to Professor Huai L. Feng for his critical revision of the manuscript.

REFERENCES

Aktay G, Emre MH, Polat A. 2011. Influence of dihydropyridine calcium antagonist nitrendipine on benzo(a)pyrene-induced oxidative stress. Arch Pharm Res 34:1171–1175.

Al-Saleh I, Alsabbahen A, Shinwari N, Billedo G, Mashhour A, Al-Sarraj Y, Mohamed Gel D, Rabbah A. 2013. Polycyclic aromatic hydrocarbons (PAHs) as determinants of various anthropometric measures of birth outcome. Sci Total Environ 444:565–578.

Bhakkiyalakshmi E, Shalini D, Sekar TV, Rajaguru P, Paulmurugan R, Ramkumar KM. 2014. Therapeutic potential of pterostilbene against pancreatic beta-cell apoptosis mediated through nrf2. Br J Pharmacol 171:1747–1757.

Chao XJ, Chen ZW, Liu AM, He XX, Wang SG, Wang YT, Liu PQ, Ramassamy C, Mak SH, Cui W, Kong AN, Yu ZL, Han YF, Pi RB. 2014. Effect of Tacrine-3-caffeic acid, a novel multifunctional anti-alzheimer's dimer, against Oxidative-Stress-induced cell death in ht22 hippocampal neurons: Involvement of nrf2/HO-1 pathway. CNS Neurosci Ther 20:840–850.

Checker R, Patwardhan RS, Sharma D, Menon J, Thoh M, Bhilwade HN, Konishi T, Sandur SK. 2012. Schisandrin B exhibits anti-inflammatory activity through modulation of the redox-sensitive transcription factors nrf2 and NF-κB. Free Radic Biol Med 53:1421–1430.

Chen R, Qiu W, Liu Z, Cao X, Zhu T, Li A, Wei Q, Zhou J. 2007. Identification of JWA as a novel functional gene responsive to environmental oxidative stress induced bybenzo[a]pyrene and hydrogen peroxide. Free Radic Biol Med 42:1704–1714.

Chiu PY, Chen N, Leong PK, Leung HY, Ko KM. 2011. Schisandrin B elicits a glutathione antioxidant response and protects against apoptosis via the redox-sensitive ERK/nrf2 pathway in h9c2 cells. Mol Cell Biochem 350:237–250.

Ding K, Wang H, Xu J, Li T, Zhang L, Ding Y, Zhu L, He J, Zhou M. 2014. Melatonin stimulates antioxidant enzymes and reduces oxidative stress in experimental traumatic brain injury: the Nrf2-ARE signaling pathway as a potential mechanism. Free Radic Biol Med 73C:1–11.

Dinkova-Kostova AT. 2013. Chemoprotection against cancer by isothiocyanates: A focus on the animal models and the protective mechanisms. Top Curr Chem 329:179–201.

Einaudi L, Courbiere B, Tassistro V, Prevot C, Sari-Minodier I, Orsiere T, Perrin J. 2014. In vivo exposure to benzo(a)pyrene induces significant DNA damage in mouse oocytes and cumulus cells. Hum Reprod 29:548–554.

Gao M, Li Y, Long J, Shah W, Fu L, Lai B, Wang Y. 2011. Induction of oxidative stress and DNA damage in cervix in acute treatment with benzo[a]pyrene. Mutat Res 719:52–59.

Gao B, Doan A, Hybertson BM. 2014. The clinical potential of influencing nrf2 signaling in degenerative and immunological disorders. Clin Pharmacol 6:19–34.

Huang HC, Nguyen T, Pickett CB. 2002. Phosphorylation of nrf2 at Ser-40 by protein kinase C regulates antioxidant response element-mediated transcription. J Biol Chem 277:42769–42774.

Ji K, Xing C, Jiang F, Wang X, Guo H, Nan J, Qian L, Yang P, Lin J, Li M, Li J, Liao L, Tang J. 2013. Benzo[a]pyrene induces oxidative stress and endothelial progenitor cell dysfunction via the activation of the NF-κB pathway. Int J Mol Med 31:922–930.

Jules GE, Pratapb S, Rameshc A, Hood DB. 2012. In utero exposure to benzo(a)pyrene predisposes offspring to cardiovascular dysfunction in later-life. Toxicology 295:56–67.

Kansanen E, Kivelä AM, Levonen AL. 2009. Regulation of Nrf2-dependent gene expression by 15-deoxy-delta12,14-prostaglandin j2. Free Radic Biol Med 47:1310–1317.

Kensler TW, Wakabayashi N, Biswal S. 2007. Cell survival responses to environmental stresses via the Keap1-Nrf2-ARE pathway. Annu Rev Pharmacol Toxicol 47:89–116.

Lacoste S, Rochette PJ, Drouin R. 2010. Mapping DNA damage to understand somatic mutagenesis. Med Sci (Paris) 26:193–200.

Leinonen HM, Ruotsalainen AK, Määttä AM, Laitinen HM, Kuosmanen SM, Kansanen E, Pikkarainen JT, Lappalainen JP, Samaranayake H, Lesch HP, Kaikkonen MU, Ylä-Herttuala S, Levonen AL. 2012. Oxidative stress-regulated lentiviral TK/GCV gene therapy for lung cancer treatment. Cancer Res 72:6227–6235.

Leong PK, Chiu PY, Chen N, Leung H, Ko KM, 2011. Schisandrin B elicits a glutathione antioxidant response and protects against apoptosis via the redox-sensitive ERK/nrf2 pathway in aml12 hepatocytes. Free Radic Res 45:483–495.

Leong PK, Chiu PY, Ko KM. 2012. Prooxidant-induced glutathione antioxidant response in vitro and in vivo: A comparative study between schisandrin B and curcumin. Biol Pharm Bull 35:464–472.

Lewtas J. 2007. Air pollution combustion emissions: Characterization of causative agents and mechanisms associated with cancer, reproductive, and cardiovascular effects. Mutat Res 636:95–133.

Li J, Ichikawa T, Janicki JS, Cui T. 2009. Targeting the nrf2 pathway against cardiovascular disease. Expert Opin Ther Targets 13:785–794.

Lin X, Yang H, Zhou L, Guo Z. 2011. Nrf2-dependent induction of nqo1 in mouse aortic endothelial cells overexpressing catalase. Free Radic Biol Med 51:97–106.

Lin F, Yu X, Zhang X, Guo Y, Huang Y, Zhou J, Zeng P, Ye D, Huang Y. 2013. A synthetic analog of lipoxin a4 partially alleviates dexamethasone-induced fetal growth restriction in rats. Placenta 34:941–948.

Liu GT. 1989. Pharmacological actions and clinical use of fructus schizandrae. Chin Med J (Engl) 102:740–749.

Luo C, Urgard E, Vooder T, Metspalu A. 2011. The role of COX-2 and nrf2/ARE in anti-inflammation and antioxidative stress: Aging and anti-aging. Med Hypotheses 77:174–178.

Nebert DW, Shi Z, Gálvez-Peralta M, Uno S, Dragin N. 2013. Oral benzo[a]pyrene: Understanding pharmacokinetics, detoxication, and consequences–cyp1 knockout mouse lines as a paradigm. Mol Pharmacol 84:304–313.

Nguyen PM, Park MS, Chow M, Chang JH, Wrischnik L, Chan WK. 2010. Benzo[a]pyrene increases the nrf2 content by downregulating the keap1 message. Toxicol Sci 116:549–561.

Pakala SB, Bui-Nguyen TM, Reddy SD, Li DQ, Peng S, Rayala SK, Behringer RR, Kumar R. 2010. Regulation of NF-κB circuitry by a component of the nucleosome remodeling and deacetylase complex controls inflammatory response homeostasis. J Biol Chem 285:23590–23597.

Perera FP, Tang D, Wang S, Vishnevetsky J, Zhang B, Diaz D, Camann D, Rauh V. 2012. Prenatal polycyclic aromatic hydrocarbon (PAH) exposure and child behavior at age 6-7 years. Environ Health Perspect 120:921–926.

Pratt MM, King LC, Adams LD, John K, Sirajuddin P, Olivero OA, Manchester DK, Sram RJ, DeMarini DM, Poirier MC. 2011. Assessment of multiple types of DNA damage in human placentas from smoking and nonsmoking women in the czech republic. Environ Mol Mutagen 52:58–68.

Satoh T, McKercher SR, Lipton SA. 2014. Reprint of: Nrf2/ARE-mediated antioxidant actions of pro-electrophilic drugs. Free Radic Biol Med 66:45–57.

Sehgal A, Kumar M, Jain M, Dhawan DK. 2012. Piperine as an adjuvant increases the efficacy of curcumin in mitigating benzo(a)pyrene toxicity. Hum Exp Toxicol 31:473–482.

Singh B, Chatterjee A, Ronghe AM, Bhat NK, Bhat HK. 2013. Antioxidant-mediated up-regulation of ogg1 via nrf2 induction is associated with inhibition of oxidative DNA damage in estrogen-induced breast cancer. BMC Cancer 13:253–261.

Tang D, Li TY, Liu JJ, Chen YH, Qu L, Perera F. 2006. PAH-DNA adducts in cord blood and fetal and child development in a chinese cohort. Environ Health Perspect 114:1297–1300.

Xie Y, Abdallah ME, Awonuga AO, Slater JA, Puscheck EE, Rappolee DA. 2010. Benzo(a)pyrene causes prkaa1/2-dependent id2 loss in trophoblast stem cells. Mol Reprod Dev 77:533–539.

Xie Y, Mao Y, Xu S, Zhou H, Duan X, Cui W, Zhang J, Xu G. 2015. Heme-heme oxygenase1 system is involved in ammonium tolerance by regulating antioxidant defence in oryza sativa. Plant Cell Environ 38:129–143.

Xu C, Yuan X, Pan Z, Shen G, Kim JH, Yu S, Khor TO,Li W, Ma J, Kong AN. 2006. Mechanism of action of isothiocy-anates: The induction of ARE-regulated genes is associated with activation of ERK and JNK and the phosphorylation and nuclear translocation of nrf2. Mol Cancer Ther 5:1918–1926.

Wang L, Wang R, Jin M, Huang Y, Liu A, Qin J, Chen M, Wen S, Pi R, Shen W. 2014. Carvedilol attenuates 6-Hydroxydopamine-induced cell death in pc12 cells: Involvement of akt and nrf2/ARE pathways. Neurochem Res 39:1733–1740.

Wu J, Hou H, Ritz B, Chen Y. 2010. Exposure to polycyclic aromatic hydrocarbons and missed abortion in early pregnancy in a chinese population. Sci Total Environ 408:2312–2318.

Wu Z, Uchi H, Morino-Koga S, Nakamura-Satomura A, Kita K, Shi W, Furue M. 2014. Z-ligustilide inhibits benzo(a)pyrene-induced cyp1a1 upregulation in cultured human keratinocytes via ROS-dependent nrf2 activation. Exp Dermatol 23:260–265.